THE JOURNAL OF PHYSICAL CHEMISTRY C

Article

pubs.acs.org/JPCC

Porous Graphene Oxide/Diboronic Acid Materials: Structure and Hydrogen Sorption

Guillaume Mercier,[†] Alexey Klechikov,[†] Mattias Hedenström,[‡] Dan Johnels,[‡] Igor A. Baburin,[§] Gotthard Seifert,[§] Roman Mysyk,[∥] and Alexandr V. Talyzin*[,†]

[†]Department of Physics and [‡]Department of Chemistry, Umeå University, SE-901 87 Umeå, Sweden

[§]Theoretische Chemie, Technische Universität Dresden, Bergstraße 66b, 01062 Dresden, Germany

[∥]CIC EnergiGUNE, Arabako Teknologi Parkea, Minano 01510, Spain

Supporting Information

ABSTRACT: Solvothermal reaction of graphite oxide (GO) with benzene-1,4-diboronic acid (DBA) was reported previously to result in formation of graphene oxide framework (GOF) materials. The theoretical structure of GOFs consists of graphene layers separated by benzene-diboronic "pillars" with ∼1 nm slit pores thus providing the opportunity to use it as a model material to verify the effect of a small pore size on hydrogen adsorption. A set of samples with specific surface area (SSA) in the range of ∼50−1000 m^2/g were prepared using variations of synthesis conditions and GO/DBA proportions. Hydrogen storage properties of GOF samples evaluated at 293 and 77 K were found to be similar to other nanocarbon trends in relation to SSA values. Structural characterization of GO/DBA samples showed all typical features reported as evidence for formation of a framework structure such as expanded interlayer distance, increased temperature of thermal exfoliation, typical features in FTIR spectra, etc. However, the samples also exhibited reversible swelling in polar solvents which is not compatible with the idealized GOF structure linked by benzene-diboronic molecular pillars. Therefore, possible alternative nonframework models of structures with pillars parallel and perpendicular to GO planes are considered.

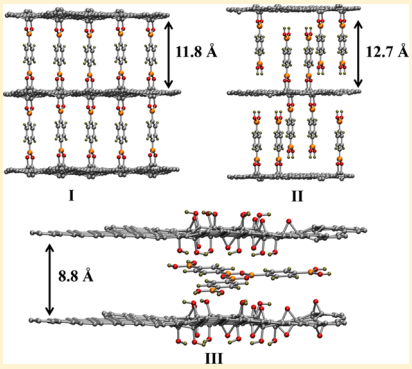

INTRODUCTION

Carbon materials have been intensively studied for hydrogen storage applications during the last two decades. The interest is maintained due to the high variety of carbon nanostructures which emerged over the years and tested for physisorption of hydrogen: activated carbons,[1,2] fullerenes,[3] carbon nanotubes,[4,5] templated and carbide-derived carbons,[6,7] and more recently, graphene-related materials.[8,9] Except for fullerenes, which are able to store hydrogen molecules in the interstices of close-packed fcc structure,[10] all other above-mentioned carbon materials adsorb molecular hydrogen proportionally to the specific surface area (SSA). The maximal uptake values seem to follow the same trends for a large variety of carbon nanostructures tested for hydrogen storage applications, both at ambient and at liquid nitrogen temperatures.[6,11−13] Approximate values of hydrogen uptake by most carbon materials can be rather well predicted knowing the BET surface area as determined using an analysis of nitrogen adsorption isotherms. The trend is approximately 2 wt % for every 1000 m^2/g at 77 K. Hydrogen uptakes at ambient temperatures do not show saturation, and experimentally evaluated wt % vs SSA trends are, e.g., ∼0.35% per 1000 m^2/g at 120 bar and ∼0.45 wt % at 300 bar.[6,12,13] Moreover, similar trends are observed for other high surface area materials, e.g., covalent organic frameworks (COFs)[14] and metal organic frameworks (MOFs).[15,16]

Gas sorption properties of graphene-related materials were rather actively studied in recent years (see, e.g., refs 9 and 17). It should be noted that initial reports on exceptionally high hydrogen uptakes by graphene-related materials[18,19] have not been confirmed in our recent studies.[20] Reduced graphene oxide (r-GO) samples produced by thermal exfoliation of graphite oxides and by KOH activation of r-GO exhibited standard correlations of hydrogen uptakes with SSA both at ambient temperature and 77 K as for other carbon nanomaterials.[20]

An increase of hydrogen uptakes can be achieved by producing materials with extremely high surface areas; e.g., our recent modeling study predicted that SSA of certain structures with highly porous graphene sheets could approach 5000 m^2/g.[21] Another parameter which has been theoretically predicted to improve hydrogen storage properties of graphene-related materials is fine-tuning of the distance between the graphene sheets.[22] Graphite shows ∼3.35 Å spacing between graphene sheets which needs to be increased by at least 3 Å

Received: July 3, 2015
Revised: October 23, 2015
Published: November 16, 2015

DOI: 10.1021/acs.jpcc.5b06402
J. Phys. Chem. C 2015, 119, 27179−27191

(diameter of a hydrogen molecule) to make the interlayers accessible for hydrogen sorption. Theoretical studies predicted that optimal separation of graphene sheets for hydrogen sorption should be on the level of 7−12 Å.[22] However, these theoretical simulations simply postulated variations of interlayer distance, while experimental realization requires some pillaring molecules or nanoparticles which could hold the graphene sheets separated from each other.

Synthesis of so-called pillared carbons has attracted significant attention in recent years due to possible applications not only for gas storage but also in supercapacitors, batteries, etc. One of the possible methods to prepare pillared layered carbon materials is to use graphite oxide as a precursor. Graphite oxides exhibit interlayer spacing of ∼6−7 Å due to extensive oxidation of graphene sheets with mostly hydroxyl and epoxy groups on the planes and carboxyl and carbonyl groups at the edges.[23,24] The structure and properties of graphite oxides depend significantly on the oxidation method,[25] and the most commonly used are Brodie[26] and Hummers methods.[27] It is known also that oxidation is not homogeneous, giving less and more oxidized regions randomly distributed over the surface area of the GO flakes.[28] Despite increased distance between GO sheets, graphite oxides exhibit negligible BET surface area due to the absence of interconnected pore networks. However, the whole surface area is accessible for liquids and solutions due to the ability of graphite oxide structure for swelling in common polar solvents.[29−31] For example, it is known that graphite oxides can be intercalated with 2−3 layers of water or alcohols, and the amount of inserted solvent is strongly dependent on the temperature.[32−34] As a result, there is a theoretical possibility to insert certain pillaring molecules between GO sheets using their solutions in polar solvents, chemically attach them to some functional groups, and after removal of the trapped solvent create networks of pores accessible for penetration of gases.

This concept was used in solvothermal reaction of graphite oxide powder with 1,4-benzene diboronic acid (DBA) which results in formation of a porous material.[35,36] To explain the relatively high SSA, the authors of this study suggested an idealized structural model where DBA molecules link neighboring graphene sheets providing layer separations of about 1−1.1 nm and named it as graphene oxide framework (GOF) (Figure 1).[35] This structure was further analyzed in several other theoretical studies,[37] including more "realistic" models which include only partly reduced and significantly curved graphene oxide sheets linked by DBA molecules.[38] It is obvious also that DBA molecules can be attached to GO planes by less than four covalent bonds, especially taking into account nonhomogeneous distribution of functional groups over GO sheets.[39] Several other linker molecules have also been tested for preparation of GOFs.[40−42] Experimental SSA reported for all so far reported GOF materials (∼400−500 m^2/g) is significantly higher compared to pristine graphite oxide but at the same time relatively low compared to other high surface area carbons (up to 3000−3500 m^2/g)[6] and the theoretical value of SSA for graphene (∼2650 m^2/g). The surface area of GOF samples is more similar to thermally or chemically reduced graphene oxides.[20,43] Hydrogen adsorption properties of GOF based on DBA linkers were reported to be superior compared to other carbon materials with similar SSA values but only at 77 K and low H_2 pressures up to 1 bar.[35] Therefore, there is strong interest to produce GOFs with higher SSA values, to tune their structure for improved gas storage applications, and to verify hydrogen storage parameters of graphite oxide/DBA materials at higher pressures and for a broader interval of SSA values.

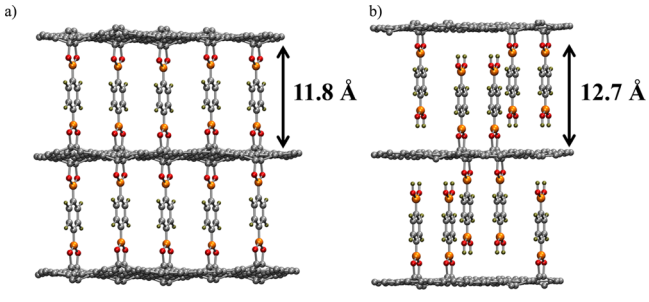

Figure 1. Idealized structural models of materials obtained using reaction of DBA with GO: (a) Scheme of "GOF" structure as suggested in ref 35. (b) Structure model with pillaring DBA units but absence of cross-linking of GO planes.

EXPERIMENTAL SECTION

Commercial graphite by Alfa Aesar (natural powder, 200 mesh, 99.9999%) was used as starting material for the preparation of graphite oxide samples by following the Hummers method (H-GO).[27] Characterization by XRD, FTIR, TGA, and XPS confirmed the high quality of samples and the absence of unreacted graphite impurities. A C/O = 2.63 composition was determined by XPS. A Brodie graphite oxide (B-GO) sample was synthesized using a graphite sample provided by Graphexel Ltd. (natural fine flake, 0−200 μm, >99.5%. Two oxidative treatments[26] have been successively applied to obtain the B-GO sample with C/O = 2.55.

Graphene oxide framework (GOF) samples were prepared by a solvothermal synthesis method[34] using the as-synthesized GO (Hummers and Brodie GO samples). Precursor GO powder (typically 200 mg) and benzene-1,4-diboronic acid (DBA) were mixed with various weight ratios (1:1, 1:3, and 1:6) in a stainless steel reactor, and methanol (10 mL) was added. The reactor was closed under nitrogen and annealed at 90 °C for different periods of time: 4−96 h. The reaction mixture was centrifuged (4400 rpm for 15 min) in order to separate the powder from the remaining methanol solution. The unreacted DBA was removed by repeated washing with methanol. The sample was finally dried under vacuum at room temperature for at least 12 h.

The reference sample of mesoporous carbon (CMK-3) was purchased from ACS Material (Medford, MA, USA). According to specifications the sample has ordered pores with size ∼3.9 nm and was synthesized by using mesoporous SBA-15 silica as the hard template.

The as-synthesized GO/DBA samples were characterized by thermal gravimetric analysis (TGA), nitrogen sorption, X-ray diffraction (XRD), X-ray photoelectron (XPS), and FTIR, and selected samples were studied by solid-state nuclear magnetic resonance (NMR) spectroscopies.

TGA was done by using a Mettler Toledo TGA/DSC1 STARe System. Experiments were performed from room temperature to 700 °C at a heating rate of 5 °C/min under nitrogen as an inert gas (50 mL/min).

The nitrogen sorption isotherms were measured using a Quantachrome Nova 1200e (surface area and pore size analyzer) apparatus at liquid nitrogen temperature. To enable the analysis of the narrowest micropores, especially in the

DOI: 10.1021/acs.jpcc.5b06402
J. Phys. Chem. C 2015, 119, 27179−27191

subnanometer region, nitrogen adsorption isotherms were also acquired using a Micromeritics ASAP 2460 analyzer supplied with a turbo-pump allowing one to start isotherm acquisition at p/p_0 values specific to micropore filling, i.e., at $p/p_0 \sim 10^{-7}$. Samples were degassed under vacuum at 120 °C (temperature was increased in steps of 20 °C) for at least 12 h. As the samples can be considered as microporous, the relative pressure range for the calculation of (BET) specific surface area was determined by plotting the adsorption isotherm as $V(1 - P/P_0) = f(P/P_0)$. The selected relative pressure range should correspond to the part for which $V(1 - P/P_0)$ continuously increases with P/P_0.[44] The slit-pore NLDFT and slit-pore QSDFT equilibrium models were applied to evaluate the cumulative surface area, pore volume, and pore size distribution.

A Siemens D5000 X-ray diffractometer with Cu Kα radiation (λ = 1.5418 Å) was used to record the diffraction patterns of pristine GO/DBA samples and after degassing under vacuum at 120 °C. Some samples were also characterized using synchrotron radiation XRD at the I711 beamline of Max IV laboratory (λ = 0.98987 Å). The XRD images were collected using a 0.7 mm capillary loaded with powder and excess of liquid solvent in transmission geometry. The images were integrated using the FIT2D software.

XPS spectra were recorded with a Kratos Axis Ultra electron spectrometer equipped with a delay line detector. A monochromated Al Kα source operated at 150 W, a hybrid lens system with a magnetic lens, providing an analysis area of 0.3 × 0.7 mm, and a charge neutralizer were used for the measurements. The binding energy scale was adjusted with respect to the C 1s line of aliphatic carbon, set at 285.0 eV. All spectra were processed with the Kratos software.

FTIR spectra were collected using a Bruker IFS 66v/S in diffuse reflectance mode.

Hydrogen adsorption was measured at room temperature using a Rubotherm gravimetric system (see details elsewhere).[10] The precision of weight measurement using the balance is ±0.01 mg, and temperature is controlled with 0.1° precision. The measurement procedure includes "zero-point correction" applied every 2 min which allows us to exclude systematic errors due to drifts. Isotherms were recorded under H_2 pressures up to 120 bar with typical sample size of 100−300 mg. Degassing of samples prior to H_2 tests was usually performed at high vacuum conditions at 120 °C for 12−16 h. On every step of the hydrogen adsorption isotherm the temperature and pressure were stabilized for ∼15 min using a circulation liquid thermostat. The precision in measured uptake values is estimated to be ±0.02 wt % for a typical 200 mg sample based on instrumental errors of the weight and temperature sensors. FLUIDCAL software was used for the calculations of fluid density of hydrogen and helium. Detailed analysis of error sources and methods of their accounting for a similar gravimetric system can be found elsewhere.[45] The H_2 adsorption tests were also performed using a Hiden Isochema Intelligent Manometric Instrument (IMI),[4647] volumetric system at ambient temperatures and at 77 K (liquid nitrogen immersion cell). Extensive studies of hydrogen storage properties vs BET surface area are available for many carbon materials for both ambient and liquid nitrogen temperatures which makes it easier to compare the sorption properties of "GOFs".

^{13}C and ^{11}B NMR spectra were recorded on a Bruker 500 MHz (^1H frequency) Avance III spectrometer equipped with a 4 mm MAS probe. All spectra were recorded at ambient temperature and with 10 kHz spinning frequency. ^1H decoupling was facilitated using a tppm15 decoupling sequence with a decoupling pulse of 5 μs for both the ^{13}C and ^{11}B experiments. ^1H decoupled ^{13}C spectra were recorded by adding 7500 scans with a 10 s relaxation delay between scans and an acquisition time of 27 ms, resulting in a total experimental time of approximately 20 h. The spectral width was set to 300 ppm. 12 000 scans and 256 scans were used for the ^{11}B NMR experiment on GO/DBA and benzene-1,4-diboronic acid, respectively. The DEPTH pulse sequence was used to suppress ^{11}B background signals.[48] All spectra were processed using Topspin 3.1 (Bruker Biospin, Rheinstetten, Germany). A Gaussian window function with lb = −10 Hz and gb = 0.01 was used for the ^{13}C spectra and an exponential window function with lb = 5 Hz for the ^{11}B spectra.

RESULTS

1. Optimization of Synthesis Conditions for Maximal SSA. The main aim of our experiments was to prepare samples with as high as possible SSA and to evaluate hydrogen storage parameters of GOFs. However, detailed characterization of produced materials (see below) proved that we successfully synthesized the same type of samples as in ref 35, but their actual structure is not compatible with the proposed model of the framework with DBA linkers connecting neighboring graphene planes. Therefore, in the following discussions we will refer to our samples as "GO/DBA", and "GOF" will only be used when the previously proposed structural model is discussed.

Several sets of experiments with variation of synthesis parameters and basic characterization were performed with the aim to increase SSA. Hydrogen sorption and structural properties of samples with the highest surface were characterized in more detail.

In agreement with earlier studies,[35] several parameters were found to affect SSA of the prepared materials: initial proportion between GO and DBA, temperature of the reaction, duration of the reaction, and the degassing temperature. Moreover, we discovered that the type of precursor graphite oxide is also of critical importance. X-ray diffraction tests demonstrated that B-GO do not react with DBA, whereas H-GO appeared to be the best and formed a single phase with expanded lattice (Figure S2) as expected from earlier reports.[34] Therefore, further experiments were performed only with the H-GO precursor.

Reaction time was optimized using a set of samples with 1:1 GO:DBA precursor ratio and a duration of the solvothermal reaction of 4, 24, 48, and 96 h. Samples prepared in this set of experiments were characterized by XRD, TGA, FTIR, and nitrogen sorption. The samples exhibited all typical features reported in earlier studies as evidence for formation of pillared GOF structure in ref 35; interlayer distance expanded by ∼3 Å (10.7 Å after 24 h treatment) compared to precursor graphite oxide (7.5 Å), signature peaks in FTIR spectra, and increased temperature of thermal exfoliation compared to pristine graphite oxide.

Maximal SSA was observed in this set of samples for the sample annealed for 24 h (∼310 m^2/g). Shorter duration of treatment was found to result in incomplete conversion of GO into the expanded phase, while too long treatment leads to collapse of the porous structure due to excessive reduction of graphite oxide. The sample treated for 96 h showed SSA of only ∼56 m^2/g, significantly decreased $d(001)$ = 7.4 Å, and strong

DOI: 10.1021/acs.jpcc.5b06402
J. Phys. Chem. C 2015, 119, 27179−27191

broad peak in XRD assigned to formation of a graphite-like structure (Figure 2).

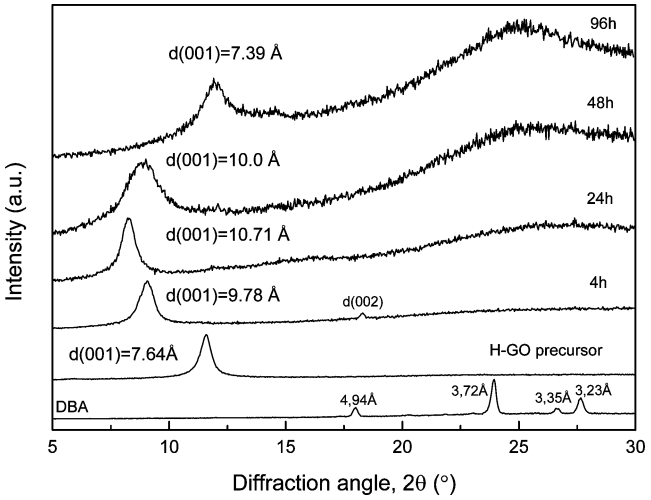

Figure 2. X-ray diffraction patterns recorded from samples prepared using variation in duration of the GO/DBA reaction (90 °C, 4–96 h). Patterns recorded from untreated GO and DBA are provided as a reference.

The next set of experiments was performed using the optimized reaction time (24 or 48 h) with variation of the GO:DBA load ratio (1:1; 1:3; 1:6). The maximal SSA in this set was observed for samples with a 1:3 ratio. Therefore, one more set of samples was prepared using the 1:3 ratio and durations of reaction of 4, 24, and 48 h. Once again, the maximal SSA was observed for the sample reacted for 24 h. Using the optimized parameters (90 °C, 1:3 GO/DBA ratio, 24 h) we prepared five samples which exhibited surface areas in the range 650–1030 m^2/g. These samples were used for a more detailed study of the GO/DBA structure and hydrogen sorption properties described in the next section.

It is necessary here to discuss in more detail how the SSA values were determined, as it is important for the evaluation of trends in H_2 uptake vs SSA. It is clear that not only errors in evaluation of H_2 uptake but also incorrectly determined SSA values could result in visible deviations from the standard trends. Figure 3 shows examples of nitrogen sorption isotherms and pore size distributions for typical GO/DBA samples. It is known that the standard BET method needs to be adjusted for microporous materials. In the case of GO/DBA samples, the BET plot is essentially nonlinear in the "standard" pressure range P/P_0 = 0,1–0,3. Moreover, linear fitting in this pressure range gives a negative intercept which proves that the SSA number obtained using this standard range of relative pressures is not valid. Therefore, using the procedure by Rouquerol et al.[44] to find a suitable range of P/P_0 is crucial. It is interesting that SSA determined using the correct relative pressure interval yields systematically higher values (by 10–30%) compared to the standard pressure range. However, we provide both numbers to compare our data with earlier studies where the

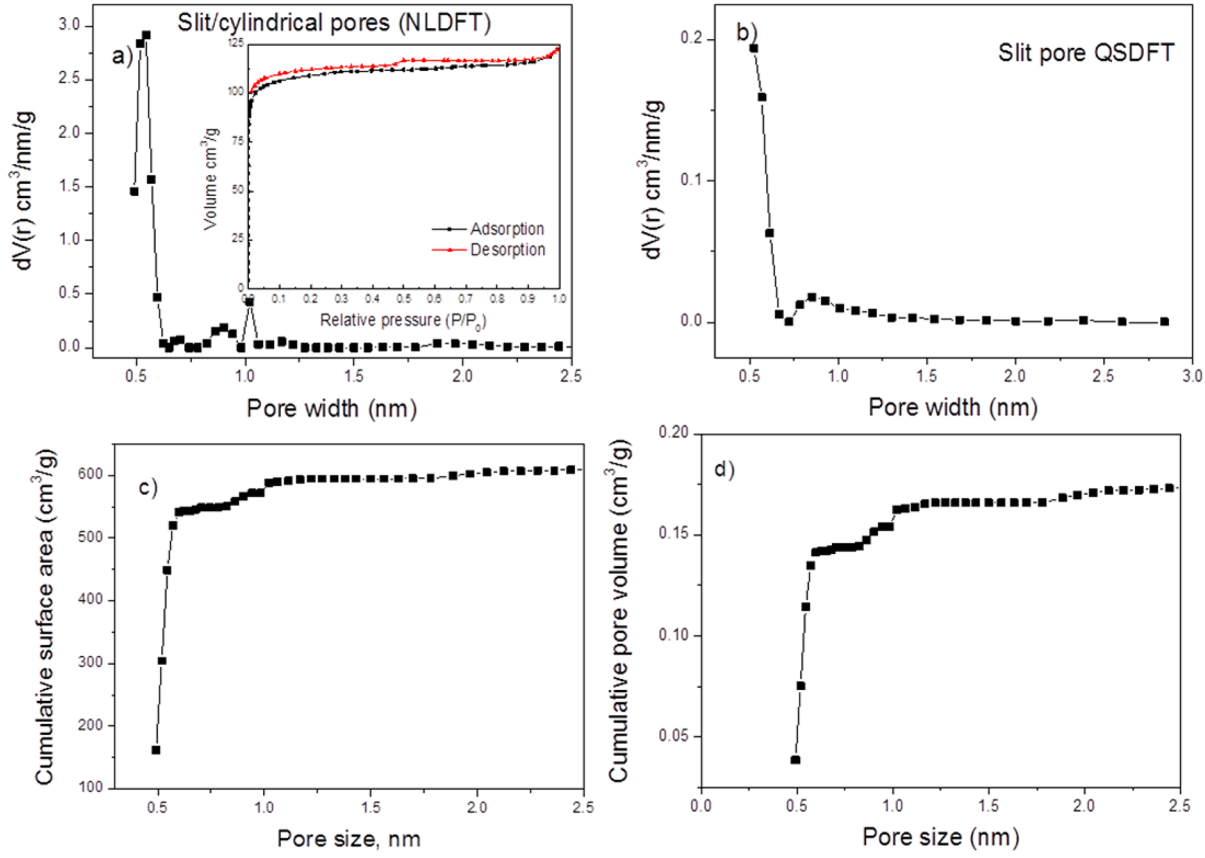

Figure 3. Pore size distribution simulated for the typical GO/DBA sample prepared using a duration of GO–DBA reaction of 24 h calculated using the NLDFT method for the slit/cylindrical pore model (inset shows nitrogen isotherm) (a) and QSDFT slit pore model (b); cumulative surface area (c) and cumulative pore volume (d) simulated using the slit pore model. The SSA value obtained for this sample using the BET method is 430 m^2/g.

DOI: 10.1021/acs.jpcc.5b06402
J. Phys. Chem. C 2015, 119, 27179–27191

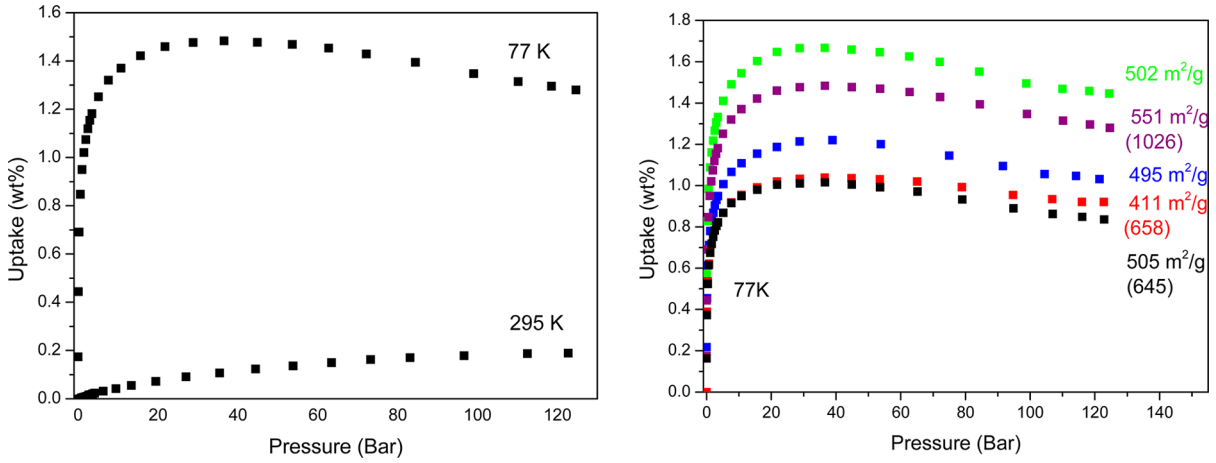

Figure 4. (a) Hydrogen isotherms for the GO/DBA sample with SSA values estimated before and after H_2 test as 1030 and 550 m^2/g, respectively. (b) Isotherms recorded from several GO/DBA samples with SSA values measured after H_2 tests and before H_2 tests when available. All SSA values were determined using P/P_0 interval <0.1 (see text).

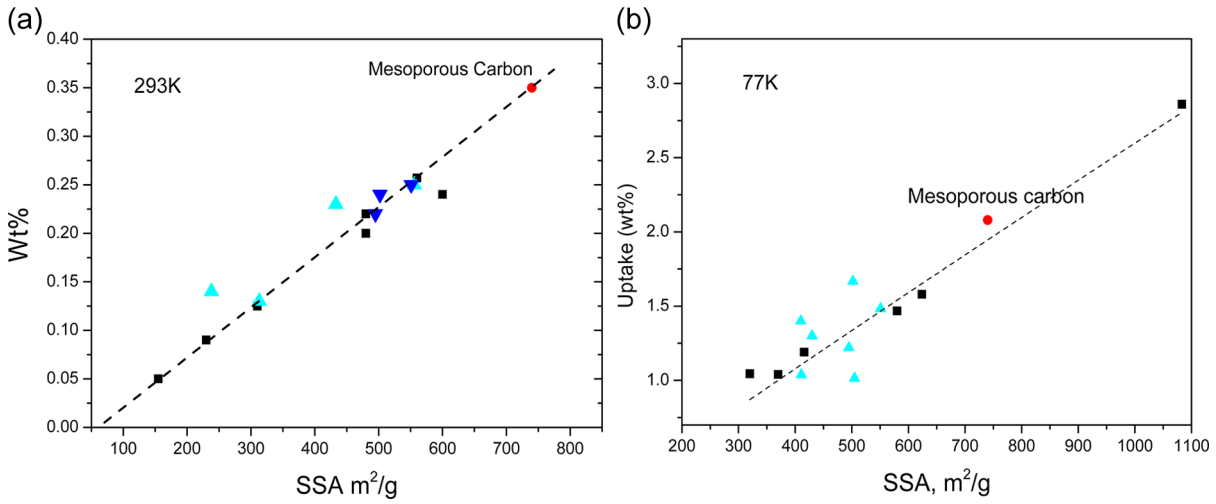

Figure 5. Values of H_2 uptakes plotted vs SSA measured at (a) ambient temperature using gravimetric (turquoise ▲) and volumetric (blue ▼) methods, as compared to r-GO samples[20] (black ■) and sample of mesoporous carbon (red ●) and (b) at 77 K using the volumetric method. Dashed lines show general trends for H_2 uptakes vs SSA for graphene-related materials[20] which are also well correlated to the trends reported for other carbon materials.[12]

exact procedure for the calculation of BET surface area was not described and likely was determined using P/P_0 = 0.1−0.3.

The maximal SSA found in our experiments was ∼1030 m^2/g, and the pore volume was ∼0.38 cm^3/g assuming the slit pore model. However, the highly porous structure is found to be unstable under the conditions of sorption measurements (up to 120 bar H_2 pressure). Measurements performed after H_2 sorption tests showed systematically lower SSA values compared to freshly prepared samples. If two sorption tests were performed using both gravimetric and volumetric methods, the SSA was found to decrease after each of these steps.

Analysis of nitrogen isotherms for pore size distribution shows (Figure 3 and Figure 1S in SI) a rather narrow distribution of pores with size below 2 nm. Most of the pore volume and surface area originate from pores with diameter below ∼1 nm. This pore size distribution is consistent with an interlayer distance of GO/DBA found by XRD methods. Fitting the experimental isotherm using a cylindrical pore model gives a main peak at ∼1 nm pore width (not shown), while for the slit pore model or slit/cylindrical models the main peak found by both QSDFT and NLDFT models is about 0.5 nm. Considering the layered structure of the studied material, using slit or slit/cylindrical models is more appropriate. Note also that the cumulative surface area of the sample shown in Figure 3 is about 540 m^2/g, higher than SSA obtained by the BET method. The BET method is known to give underestimated SSA values for ultramicroporous carbons.[49] However, due to the traditional use of the BET calculation and to enable comparison with the literature, the following discussion is based on BET SSA.

2. Hydrogen Sorption Results. Examples of hydrogen sorption isotherms recorded at 293 and 77 K for several GOF samples with high SSA are shown in Figure 4. However, the SSA of this sample had dropped from ∼1030 m^2/g measured before the H_2 test to ∼550 m^2/g measured after the test. A significant drop of SSA values after H_2 tests (∼20−50%) was observed for several GOF samples. As verified in our experiments, the change of SSA is likely to be connected to pressure-induced pore network collapse. The higher the initial

DOI: 10.1021/acs.jpcc.5b06402
J. Phys. Chem. C 2015, 119, 27179−27191

SSA was, the stronger was also the decrease due to pressure effects. Note that every H_2 or nitrogen sorption test was preceded by vacuum degassing steps at 120 °C for 10−16 h, and the decrease of SSA could be a result of prolonged annealing. However, repeated vacuum degassing at this temperature alone was typically not observed to result in lower SSA numbers. Moreover, we performed a set of experiments where SSA was measured for the GOF sample at progressively higher temperatures in the range 20−120 °C. As expected, the highest surface area was measured after degassing at 120 °C. Repeated degassing with longer duration (up to 24 h) did not result in pore collapse, and the SSA values did not decrease. Therefore, the decrease of the SSA should be connected to partial collapse of the porous structure due to high pressures of the H_2 gas (up to 120 bar) used in our experiments. A similar effect was previously reported for some MOF materials as a result of applying high gas pressure.[16] To verify the effect of pressure we performed experiments with hydrogen isotherms recorded at 77 K with progressively increased pressure. The maximal pressure for the first isotherm was ∼20 bar, for the second step 50 bar, and for the third step 120 bar and finally at ∼20 bar again with degassing intermissions (Figure 6S in SI). No obvious decrease of H_2 uptake was observed, but the SSA measured before and after the experiments decreased by ∼20%. Therefore, the partial collapse of the pore network had to occur already at pressures below 20 bar.

Figure 5 shows a summary of hydrogen sorption experiments performed with several GO/DBA samples at 293 and 77 K as compared with our earlier hydrogen sorption results obtained on reduced graphene oxide. The SSA values obtained after H_2 tests were used for this figure. It is clear that GO/DBA samples demonstrate hydrogen uptake that correlates with SSA and follows the standard trend of other carbon materials both at ambient and at liquid nitrogen temperatures (∼2 wt % per 1000 m^2/g of SSA). Stronger than usual scatter of points with similar SSA values should be attributed to the effect of pressure-induced pore collapse which makes the true value at the moment of H_2 isotherm recording somewhat uncertain.

In agreement with earlier reports, the hydrogen isotherms recorded at 77 K show rather steep increase at low pressures. For example, the isotherm shown in Figure 4 reached 0.8 wt % at 1 bar H_2 pressure with saturation value of ∼1.48 wt %. Hydrogen uptake values observed in our study are in good agreement with earlier observations which reported 1.2 wt % for a sample with SSA of 470 m^2/g.[35,36] Note that the SSA was not verified after H_2 tests in the earlier studies and even for pristine samples was provided using an unspecified P/P_0 interval.

It is interesting to note that maximal SSA values observed for r-GO and GO/DBA samples are nearly identical. However, r-GO samples are amorphous and exhibit broader pore size distribution. Crystalline packing of GO layers in the GO/DBA structure and the narrow pore size distribution can be an advantage for, e.g., membrane applications of this material. However, for hydrogen storage applications the SSA of the materials needs to be increased significantly. Advantages and limitations of GO/DBA materials to produce materials with even higher SSA can be verified only if the structure of the resulting materials is reliably established. However, detailed characterization data presented below demonstrate that the GOF structure proposed in earlier studies cannot explain some properties of the materials obtained by solvothermal reaction of GO with DBA.

3. Structure of GOF Samples: No Covalent Linking of GO Layers. Analysis of the samples prepared using solvothermal reaction of GO powder with DBA was performed using XRD, TGA, FTIR, XPS, BET surface area, and pore size distribution analysis and confirms that we synthesized the same material as reported by J.Burress et al.[35] The main features reported as typical for GOF material were also found in our samples: sizable SSA over 400 m^2/g, expansion of lattice compared to GO by ∼2.5−3 Å, typical peaks in FTIR assigned to B−O bonds, and the presence of boron proved by XPS and NMR spectroscopy. However, we report here additional characterization of these samples which is not compatible with the idealized GOF structure suggested in earlier studies.

The GO/DBA samples described in the previous section were characterized by XRD to evaluate the change of interlayer distance due to insertion of DBA molecules into the GO structure. The air-dried GO/DBA samples showed an expansion of interlayer distance from ∼7.5 Å (for pristine air-exposed samples) up to 10−11 Å. Vacuum drying at 120 °C (degassing conditions for BET and H_2 sorption tests) resulted in a further decrease of $d(001)$ to values in the range 9.5−9.7 Å. However, the lattice expansion observed for our GO/DBA samples does not show a precise correlation with SSA values, and variations up to ∼300 m^2/g were observed for samples with almost the same $d(001)$ values of interlayer distance. The XRD method provides a value of interlayer distance averaged not only over thousands of interlayers (interstratification) but also over the variations within each interlayer (intrastratification). Moreover, removing guest methanol molecules from the pore network can also be inhomogeneous, e.g., if some interlayers are not efficiently emptied or collapsed in the process of solvent removal. The 0.1−1 Å variations of $d(001)$ observed in our experiments originate from some layers which are not filled by linker molecules or collapsed due to an excessive duration of the reaction. Therefore, the absence of a precise correlation between SSA values and the value of $d(001)$ is not surprising. A significant drop of SSA is observed only when $d(001)$ decreases below 9.4 Å. Nevertheless, it is clear that a sizable surface area is observed for samples with interlayer distance expanded by 2−3 Å compared to the precursor GO.

The higher interlayer distance found in GO reacted with DBA under solvothermal conditions was interpreted in earlier studies as evidence for the idealized theoretically predicted GOF structure.[35] The hypothetical GOF structure consists of graphene layers (assuming complete reduction of graphene oxide) and DBA molecules serving as pillars covalently attached to graphene. However, our experiments prove that the GOF model cannot be applied to the GO/DBA samples since it is not compatible with the observed swelling in polar solvents (Figure 6).

Several GOF samples were tested by X-ray diffraction in liquid methanol and showed a swelling of the structure with a lattice expansion of ∼3.5−4 Å, which corresponds to insertion of one methanol monolayer (see Figure 6). Moreover, GOF samples also swell in water with $d(001)$ increasing up to ∼15.3 Å, which corresponds to an ∼5 Å increase which is the size of approximately two water monolayers. Therefore, the air-exposed samples will also absorb a significant amount of water proportional to the humidity levels, similar to the precursor graphite oxides. It can be concluded that GOF samples exhibit swelling behavior very similar to the one which

DOI: 10.1021/acs.jpcc.5b06402
J. Phys. Chem. C 2015, 119, 27179−27191

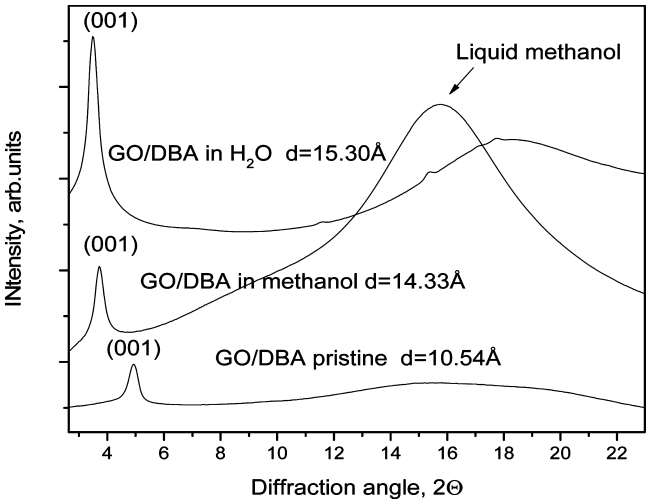

Figure 6. X-ray diffraction patterns recorded from GO/DBA samples in pristine air exposed state, in excess of liquid methanol, and in excess of water (λ = 0.98987 Å). The pristine state is recovered after solvent evaporation at ambient temperature.

we earlier reported for the precursor graphite oxides,[25,33] thus ruling out the possibility of covalent linking between GO layers. The pillaring units in hypothetical GOF structure are perpendicular to the graphene planes. Therefore, a further increase of interlayer distance due to absorption of water or methanol is not expected without breaking the covalent bonding between DBA units and graphene sheets. Strong curvature of graphene sheets is also unrealistic and anyway ruled out by the presence of well-defined d(001) reflection in XRD. Note that a similar reaction was observed earlier when diboronic acid was replaced with monoboronic acid.[36] In this case only one side of the molecule can be reacted with GO, and a covalent linking of GO sheets is impossible by definition. Nevertheless, the samples of GO reacted with diboronic and monoboronic acids showed similar expansion of the (00*l*) lattice and nearly identical surface areas (470 and 442 m^2/g, respectively). Moreover, FTIR spectra of these two materials were reported to show identical intensity of peaks assigned to B−O vibrations.[36] Therefore, the hypothetical cross-linking of GO sheets is not required to explain high SSA values and other main features of GO/DBA materials. The observed lattice expansion could be explained if DBA linkers are attached to only one of the GO planes, thus forming "pillaring" structure rather than "framework".

The absence of covalent linking of GO layers is not the only argument against the framework structure proposed in earlier studies.[35] Characterization of GO/DBA samples proves that graphene oxide layers are not reduced to graphene. Our samples showed sizable SSA only when the overall reduction of graphite oxide was relatively small, and stronger reduction caused by longer solvothermal reaction (96 h) results in significantly decreased SSA of the samples.

The effect of reaction time on the structure of GO/DBA samples was evaluated using XRD, FTIR, and TGA (Figures 7−10). The TGA traces of GO/DBA samples showed an increased exfoliation temperature compared to the precursor GO (Figure 7). First, the existence of exfoliation proves that the material remains to be graphene oxide, and it is not reduced back to graphene as in the idealized GOF structural model. The weight loss due to exfoliation can be used to evaluate the degree of sample oxidation, and by comparing it with the precursor GO it is possible to estimate how strongly the samples were reduced by the reaction with DBA under solvothermal conditions.

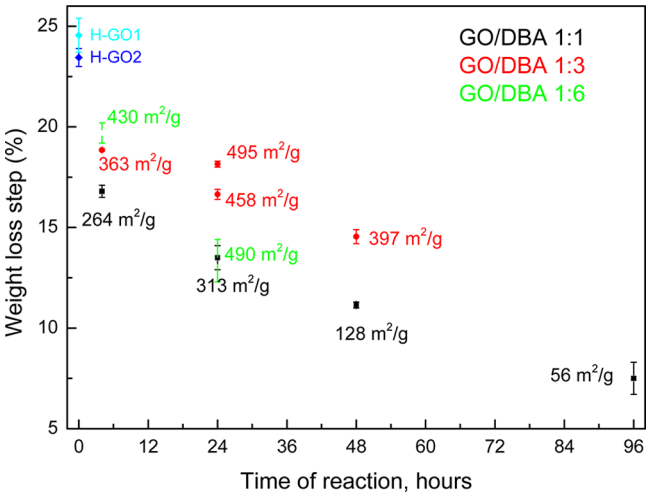

Figure 8. Effect of GO−DBA reaction time on the reduction state of GO/DBA samples and their BET surface area. The weight loss due to deflagration of GO at 180−230 °C is found using TGA traces shown in Figure 7.

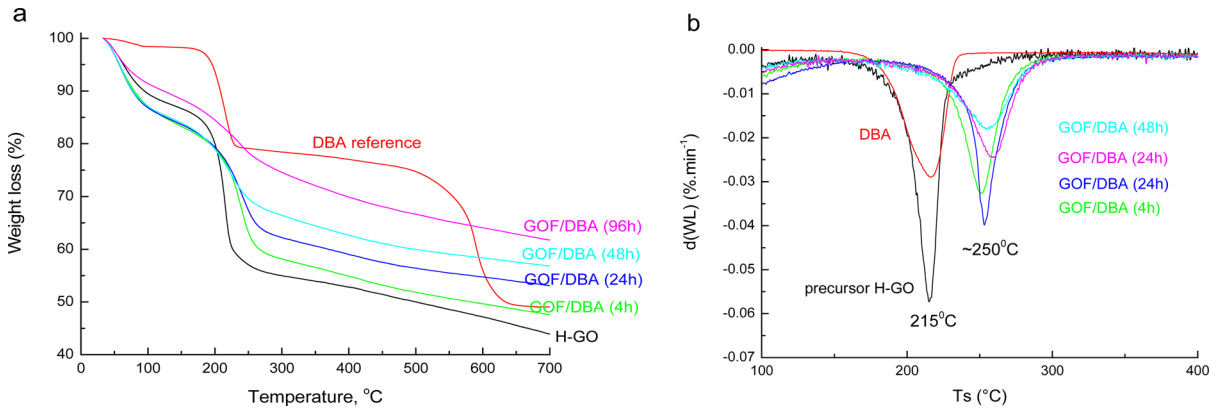

Figure 7. TGA traces for several GO/DBA samples prepared with different GO−DBA ratios and duration of reaction in (a) pristine and (b) differential form.

DOI: 10.1021/acs.jpcc.5b06402
J. Phys. Chem. C 2015, 119, 27179−27191

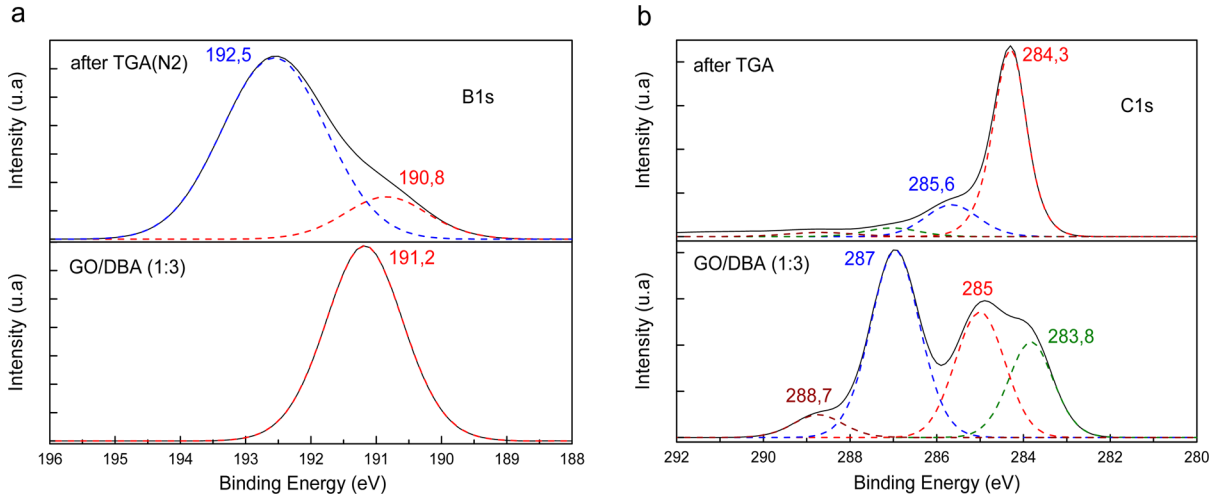

Figure 9. XPS spectra recorded from a pristine GOF sample and from a sample annealed up to 900 °C under nitrogen flow in TGA analysis: (a) spectra region of the B 1s peaks and (b) spectral region of the C 1s peak.

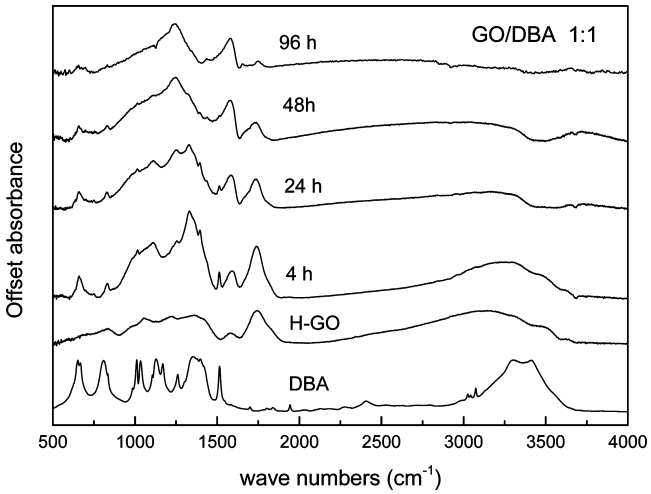

Figure 10. FTIR spectra recorded from GO/DBA samples prepared using different duration of reaction.

It is important to emphasize that an increase of the exfoliation temperature of GO/DBA materials relative to precursor graphite oxide cannot be considered as evidence for the formation of covalent links between individual GO sheets.[11] It is well-known that the exfoliation temperature of graphite oxides shows variation of ∼130° depending on the particular oxidation method used with as high as 325 °C reported for Brodie GO.[25,50] The exfoliation temperature depends on oxidation degree of the GO and proportion between the numbers of various functional groups (epoxy and hydroxyl groups first of all). The solvothermal reaction with DBA results in partial reduction of GO and change in the relative amounts of various functional groups. The change of exfoliation temperature can then be explained without any cross-linking of GO planes. Note also that a reaction of GO with monoboronic acid also results in materials with increased exfoliation temperature, whereas the cross-linking of GO planes according to the GOF model is not possible for that pillaring unit.

The degree of GO reduction clearly increases with longer duration of solvothermal treatment (Figure 8), while the maximal surface area is achieved after 24 h. The sample synthesized using a reaction duration of 96 h showed a relatively weak peak from GO/DBA in XRD with significantly decreased $d(001)$ = 7.39 Å and a broad peak due to formation of graphitic carbon and an SSA value of 56 m^2/g. This sample also shows rather small weight loss around 250 °C (temperature of exfoliation) as detected by analysis of TGA.

TGA traces of precursor H/GO samples show some weight loss mostly due to evaporation of water below ∼150 °C and a sharp weight loss step of ∼23−24 wt % at ∼215 °C due to exfoliation and release of oxygen-containing functional groups (Figure 7 a,b). The height of the weight loss step decreases almost linearly for samples with longer reaction duration (Figure 8). Smaller weight loss on the exfoliation step is evidence for a partial reduction of GO when it is transformed into GO/DBA. The maximal surface area was observed for samples reacted for 24 h and weight loss in the exfoliation step of ∼13−18 wt %. Using TGA data it can be approximately estimated that about 25−50% of the oxygen-containing groups were removed from precursor GO when the GO/DBA structure is formed.

It can be concluded that a heat treatment of graphite oxide at 90 °C in methanol solution of DBA results in slow reduction of the graphite oxide. However, if too many functional groups are removed from GO sheets, the pillared structure collapses as indicated by a decreased surface area found for samples with reaction times over 24 h.

The data presented in Figures 6−8 can be interpreted as follows: DBA pillars are attached to oxidized areas of GO sheets and provide wider separation of layers, while partial reduction is responsible for the interconnected network of "graphene" pores. Excessive reduction of GO sheets results in collapse of the porous network since the oxidized and pillaring areas are also removed in the process of reduction. Since graphene is a rather flexible material, it can be expected that separating pillaring units too far from each other will result in a collapse of slit pores with formation of a graphitic lattice.

The TGA data do not allow us to estimate how many DBA molecules were actually intercalated into the GO structure. The TGA trace of the precursor DBA shows two weight loss steps, the first one due to condensation/polymerization reaction and loss of water and the second due to a pyrolysis and formation of carbonaceous deposits. The first step should be absent in GO/

DOI: 10.1021/acs.jpcc.5b06402
J. Phys. Chem. C 2015, 119, 27179−27191

DBA samples if the DBA molecules are already reacted with GO sheets and attached to them by covalent bonds. Pyrolysis of linkers should be observed similarly to COF-1 material.[51] However, no weight loss step is observed in TGA traces of GO/DBA samples around 600 °C. Therefore, either the linkers are evaporated from the samples at the moment of GO exfoliation and the breakup of the structure or the number of intercalated DBA molecules is too small for the weight loss to be detected. It is known that exfoliation of graphite oxide has explosive character. Direct observations show that GO exfoliates with fire even when the material is thermally treated under argon. Therefore, it would not be surprising that the strong exothermal effect of GO exfoliation results also in breakup of the pillaring molecules.

In principle, one could suggest that the whole pillaring molecule is removed at the exfoliation step if the oxygen bonds to the graphene sheets break at this temperature. However, this possibility can be ruled out based on the elemental analysis performed. The amount of boron in GO/DBA structure before and after exfoliation was determined using XPS which provides a quantitative estimation of the C:O:B composition (Figure 8).

The sample with the highest SSA showed the following composition: C-68.3%, O-29%, B-2.61%. This corresponds to 1 boron per 23 carbons and ∼1 DBA molecule for 46 graphene carbons, in good agreement with earlier studies.[35] The same sample analyzed after TGA experiment (Figure 6) showed C-85.13%, O-11.16%, and B-3.71%. This corresponds to C/O = 7.6, while the boron concentration is increased by ∼50%.

Analysis of chemical shifts also confirms a reduction of the GO/DBA sample and a change of the chemical state for boron after annealing up to ∼700 °C. The B 1s peak of GO/DBA is found originally at 191.6 eV (B−OH), slightly downshifted compared to reference samples of DBA and COF-1 (191.9 and 192 eV, respectively). After heat treatment the main part of the boron is found with a peak position at 192.5 eV typical for B−O. The C 1s spectra found for GOF samples are similar to spectra of pristine GO and show several components typically assigned to epoxy, hydroxyl, and carboxylic groups as well as to graphene skeleton carbons in the unoxidized state. No specific peak due to carbons from DBA linkers is found in XPS spectra, in agreement with earlier reports on GOF characterization.

Evidence for some DBA-derived molecules in GO/DBA samples is found in FTIR spectra (Figure 10 and Supporting Information). The GOF signature peaks reported in ref 35 are found also in our FTIR spectra. These peaks are similar to spectra of pristine DBA but not entirely identical, suggesting some modification of DBA structure consistent with structural model including DBA-related pillaring unit. In agreement with XRD and TGA data, the sample treated for 96 h shows only peaks from amorphous carbon.

The presence of boron and reduction of GO in GO/DBA samples are also confirmed by solid-state ^{13}C NMR spectroscopy (Figures 11 and 12). The GOF samples showed an increased ratio of sp^2- to sp^3-carbons compared to precursor GO. We assign this change mainly to reduction, although the presence of DBA in the GO structure will increase the total amount of sp^2-carbons. According to XPS only 2.6−2.8% of B is present in GOF, and moreover, a hump (at 135 ppm) on the sp^2 peak of GO/DBA was expected to be seen if significant amounts of DBA had been incorporated into the material. Boron NMR spectroscopy shows that most of the boron atoms in the studied sample still retain sp^2 hybridization typical for

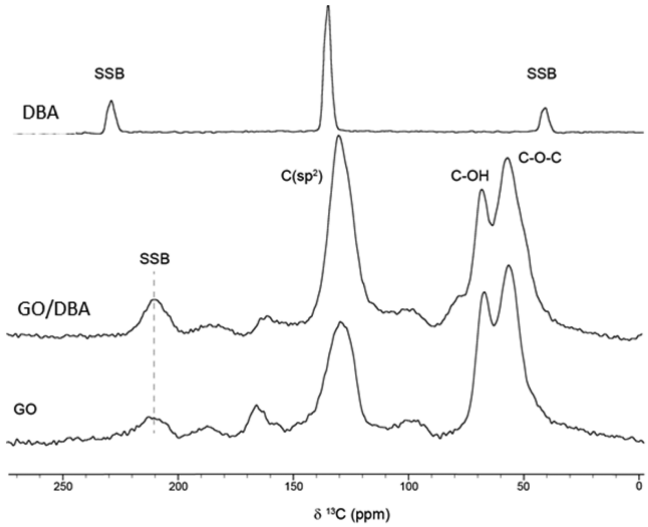

Figure 11. ^1H-decoupled ^{13}C spectra performed under magic angle spinning of benzene-1,4-diboronic acid, GO/DBA, and unmodified GO. C−OH and C−O−C refer to ^{13}C resonances originating from sp^3-hybridized carbons in tertiary alcohols (67 ppm) and epoxy groups (56 ppm), respectively. The peak from sp^2-carbons is located at 129 ppm. SSB = Spinning side-bands.

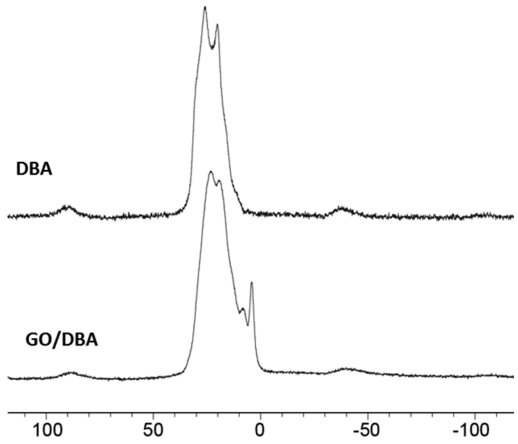

Figure 12. ^{11}B NMR of benzene-1,4-diboronic acid and l GO/DBA sample.

boronic acids or esters and a minor part of sp^3-hybridized boron atoms originating most likely from BO_3 units.

DISCUSSION

The data presented above confirm that solvothermal reaction of GO with DBA performed in methanol results in a reproducible formation of nanoporous materials with medium SSA values and typical pore size about 0.5 nm. It is evident that intercalation of GO with DBA-derived molecules does occur under conditions of solvothermal reaction. However, no firm evidence could be obtained for linking of DBA-derived molecules to neighboring graphene oxide sheets. Most of the typical signature features of this material are in good agreement with earlier studies,[35] but the structural model proposed earlier (Figure 1a) is not compatible with swelling properties of the material. The swelling of GO/DBA samples in methanol and water revealed in our experiments with an increase of d(001) by 3−5 Å is not compatible with the GOF structure where DBA units link GO graphene sheets as proposed in earlier

DOI: 10.1021/acs.jpcc.5b06402
J. Phys. Chem. C 2015, 119, 27179−27191

studies.[35] The DBA linker units in the hypothetical GOF structure must be oriented perpendicularly to the GO sheets already in the nonswelled state. Therefore, further increase of interlayer distance is impossible without breaking the covalent bonds or unrealistic elongation of DBA molecules. Moreover, the cross-linking of graphene planes according to GOF structure requires unlikely combination of four hydroxyl groups located exactly over each other on the neighboring GO sheets.

Note that the true structure of the precursor GO itself remain uncertain even after over 150 years of studies due to strong disorder, inhomogeneous distribution of functional groups over the graphene sheets, and a variety of oxygen-containing groups which can be found in GO.[23,52] Therefore, it is not surprising that DBA-modified material provides challenges for establishing the true structure of the material. For example, powder XRD data do not provide information about the nature, numbers, and orientation of functional groups in graphite oxide and GO/DBA samples. No direct information about the number or the geometry of pillaring molecules can be extracted from XRD, whereas the expansion of the interlayer distance of GO can be interpreted using rather different structural models.

As discussed above, the increased temperature of GO/DBA exfoliation cannot be considered as evidence for interlinking, as the exfoliation temperature of precursor graphite oxides is known to vary between 190 and 325 °C[50] and depends on total number and relative proportion of various oxygen-containing functional groups.[25] Partial reduction, intercalation, and chemical modification of GO are expected to result in shifts of the exfoliation temperature in the absence of cross-linking. The data obtained using characterization methods (e.g., FTIR and NMR) also cannot provide decisive evidence for GOF structure as they cannot distinguish boronate ester formation between DBA molecules from DBA attached to GO sheets. Finally, reaction of GO with monoboronic acid (which cannot serve as cross-linker) results in formation of materials with nearly identical signature features: SSA values, peaks in FTIR spectra, increased exfoliation temperature, etc.[36] It can be concluded that the theoretical GOF model with cross-linked planes suggested in previous studies[35] is not valid for experimentally prepared materials. Therefore, we suggest using a different name instead of "GOF", for example, DBA-pillared GO (DBApGO). This name will be suitable for any type of pillaring units, either parallel or perpendicularly oriented relative to the GO sheets.

Summarizing the characterization data presented above, the model of DBApGO structure must explain the following properties:

- relatively high BET surface area which originates mostly from pores with ∼0.5 nm width.
- partial reduction of graphite oxide; ∼25−50% of the functional groups are removed during the reaction with DBA.
- expanded GO lattice with typical interlayer distance of about 9.5 Å after vacuum drying. Note that swelling in water suggests that the interlayer distance measured in air is dependent on humidity and overestimated.
- presence of boron in an amount of 2.6−2.8 at %.
- the chemical state of boron is similar to the precursor DBA or boron esters.
- swelling in polar solvents.

The most obvious alternative structural model suggests that the DBA molecule is attached only to one graphene oxide sheet and not attached to the neighboring sheet. It should be noted that porous structures with very similar surface areas were found also for GO reacted with monoboronic acid.[36] This molecule has only one boron atom attached to the benzene ring, and cross-linking by covalent bonds is thus impossible. The pillaring effect of the DBA molecule attached to the graphene oxide sheet by one or two bonds (e.g., as in Figure 1b) is compatible with the observed swelling of DBApGO structure in polar solvents. However, this model does not explain the observed dependence of the surface area values on the degree of GO sheet reduction. If this model was correct, the prolonged reaction of GO with DBA is unlikely to induce a collapse of the pore network as observed in our experiments. Instead, stronger reduction of GO could be expected to result in increased surface area. Removal of oxygen improves SSA values by definition since oxygen atoms are heavier than carbons. Our data demonstrate that maximal SSA values are observed for partly reduced GO sheets, but the presence of oxidized graphene regions is essential for formation of a porous structure.

It is known that already the precursor graphene oxide is not homogeneously oxidized with some areas covered by functional groups and some (smaller) areas unoxidized.[52,53] As a result, it is also not homogeneously hydrated.[28] However, the unoxidized "graphene" areas are not interconnected in pristine graphene oxide which results in negligibly small surface area if measured by gas adsorption. It can be speculated that partial reduction of GO which occurs in the process of the solvothermal reaction results in formation of an interconnected network of "graphene capillary" formed in nonoxidized areas, while the DBA molecules are trapped in oxidized regions of GO sheets. In this part, the mechanism of pore network formation is similar to the one suggested for the formation of GOF structure.[35]

However, we suggest an alternative model where pillaring units formed by DBA molecules are not perpendicular to GO sheets as in the GOF model but approximately parallel to them and not covalently attached (Figure 13). Insertion of DBA-derived molecules parallel to GO sheets would result in expansion of the lattice by ∼3.5 Å which is in reasonable agreement with experimentally observed values of $d(001)$ = 9.0−10.5 Å. The size of "graphene capillary" formed by unoxidized areas will then be about 5−7 Å considering van der Waals distance of ∼3.5 Å typical for graphite, also in good agreement with experimental results.

The ability of DBA molecules to intercalate the GO lattice should be closely related to the swelling properties of GO in methanol. Our earlier experiments with powders immersed in methanol solution demonstrated that the interlayer distance of Hummers GO expands up to ∼13 Å due to swelling at ambient temperature.[25,33] Note that the interlayer distance is temperature dependent and could be different at the conditions of solvothermal reaction. At ambient temperature the DBA molecules dissolved in methanol enter the lattice together with solvent but escape it when the solvent is removed and the sample dried.

We speculate here that if DBA molecules react with each other inside of the GO lattice and the products of this reaction become insoluble, they can form stable pillars oriented parallel to GO sheets. For example DBA molecules could form dimers, trimers, or small fragments of COF-like structures at the

DOI: 10.1021/acs.jpcc.5b06402
J. Phys. Chem. C 2015, 119, 27179−27191

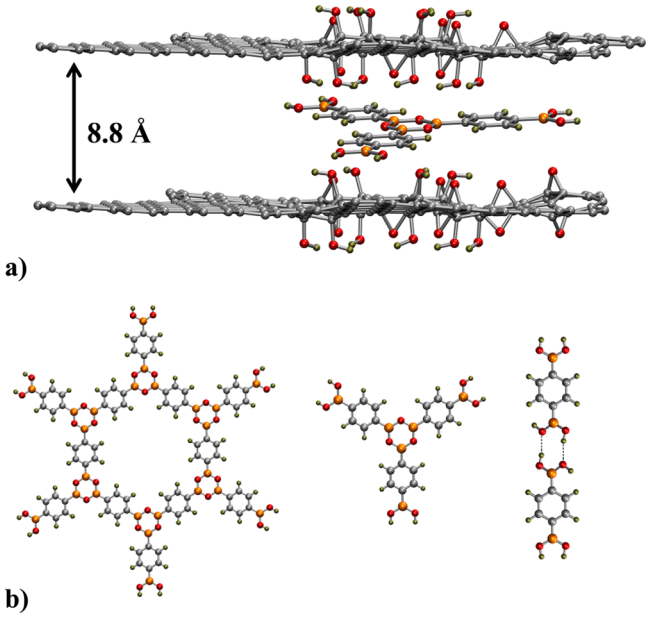

Figure 13. (a) Structural model of partly reduced GO pillared with trimeric DBA molecules. (b) Possible pillaring units constructed by DBA molecules.

conditions of synthesis (Figure 13b). Any of these units could be serving as pillars in the GO/DBA structure. Randomly distributed between GO planes, these pillaring units would be disordered and not observable with XRD. Formation of COF-like fragments under conditions of solvothermal reaction is something logical to expect. In fact, the same reaction performed using mesytilene/dioxane solvent instead of methanol is known to result in the formation of COF-1 material and expansion of the GO lattice by the same value as in methanol.[35] If methanol is used as a solvent for DBA, the formation of crystalline COF structure is not observed, but the formation of amorphous COF-like molecular fragments between GO sheets under confinement conditions can still be possible. The structural model suggested above explains several important properties observed for DBApGO samples: their swelling in polar solvents, limitation of observed SSA values to moderately high 400−1000 m^2/g, and the collapse of the porous structure upon stronger reduction (longer reaction time). If this model is true, the maximal surface area of GOF samples cannot be increased significantly: a certain proportion between areas of oxidized and unoxidized areas must be retained as too large "graphene capillars" will collapse and form a graphitic structure.

Despite the lack of precise structural information for the DBApGO samples studied here, it is interesting to discuss also the hydrogen sorption results. The microporous nature of the samples is obvious from the analysis of nitrogen sorption isotherms. We did not find a hydrogen uptake enhancement predicted by theoretical simulations for subnanometer graphene slit pores.[22] However, our results are not evidence that experiments do not confirm these predictions. Instead, one should conclude that the structure of DBApGO materials is far from the theoretically simulated graphene slit pores separated by certain interlayer distance.

First of all, the presence of oxygen functional groups is likely to affect hydrogen sorption adversely. Moreover, the shape of the pores in our DBApGO samples is uncertain, while the predictions are valid only for slit pores.[22] Characterization provided above implies irregular pores significantly deviating from a slit shape for any nonidealized structural model either with pillars or without them. Theoretical calculations performed for graphene slit pores with typical lateral size of a few nanometers imbedded between oxidized areas demonstrated that they cannot be considered as hydrophobic due to the oxygen-containing hydrophilic groups which define pore width.[54] The top and bottom graphene planes are hydrophobic, but the side walls formed by oxidized areas are hydrophilic. It can be concluded that the studied samples do not allow the verification of the theoretical simulations performed for precisely sized slit pores formed by hydrophobic graphene sheets.

The overall hydrogen storage properties of GO/DBA samples found in our experiments are far from the best examples reported for nanostructured carbon materials. Since the hydrogen sorption correlates with the SSA values following the standard trends, it is possible to predict the maximal hydrogen sorption of pillared graphene oxides using an estimation of the maximal theoretical surface area. The surface area of graphene is about 2650 m^2/g. Adding oxygen in amounts which correspond to C/O = 2.5 will result in a decrease of the theoretical SSA of GO to ∼1800 m^2/g. Adding pillaring molecules and removing ∼50%, the oxygen functional groups will once again change SSA value due to a change in molar mass of the material. However, it is clear that the theoretical surface area is below the value of graphene and unlikely to exceed 2000 m^2/g. In the absence of strong deviations from the standard trends the maximal hydrogen uptakes can be predicted using data shown in Figure 5 or a similar figure extended to higher SSA values from our earlier published data for graphene-related materials.[20,55]

CONCLUSIONS

In conclusion, we performed an optimization of the conditions for the solvothermal reaction of GO with DBA earlier reported to result in the formation of a structure pillared by benzene−diboronic linkers and named after the theoretical models as graphene oxide frameworks (GOFs). Our experiments confirm the formation of porous GO structures with SSA values up to 1000 m^2/g and subnanometer sized pore widths. However, extensive structural characterization allows us to rule out a framework structure of the studied samples with GO sheets linked by DBA units since it is not compatible with experimentally found swelling of GO/DBA material in water and methanol. The increase of interlayer distance of GO/DBA material by ∼5 Å in liquid water is impossible within the earlier proposed GOF model which suggests cross-linking of graphene sheets by covalently bound DBA units.

Therefore, only models which suggest "pillaring" of GO sheets not involving covalent cross-linking (framework) must be considered. The existing characterization data for DBA-pillared GO material are compatible with two hypothetical structures: the first model suggests DBA molecules attached only on one side of the GO interlayer, while the second alternative model assumes partly reduced GO sheets separated by COF-like fragments (e.g., dimeric or trimeric products of DBA) in parallel to the GO sheet orientation.

The hydrogen uptakes of the prepared samples follow the standard correlation with surface area. The improved hydrogen uptake properties reported in earlier studies for GOF samples with respect to surface area are not confirmed and are likely to

DOI: 10.1021/acs.jpcc.5b06402
J. Phys. Chem. C 2015, 119, 27179−27191

be due to experimental error connected to an underestimation of BET surface area. The studied material is essentially microporous, and using nitrogen sorption isotherms for evaluation of SSA requires proper selection of the P/P_0 interval for the BET plot.

■ ASSOCIATED CONTENT

Supporting Information

The Supporting Information is available free of charge on the ACS Publications website at DOI: 10.1021/acs.jpcc.5b06402.

More detailed FTIR data with table of peak positions, details of nitrogen isotherm analysis for several samples, additional XPS data, and H_2 uptake isotherms for several samples (PDF)

■ AUTHOR INFORMATION

Corresponding Author

*E-mail: alexandr.talyzin@physics.umu.se.

Notes

The authors declare no competing financial interest.

■ ACKNOWLEDGMENTS

This work was financially supported by the Swedish Research Council, Grant no. 621-2012-3654 (A.T.), and by the Graphene Flagship (contract no. NECT-ICT-604391). We thank A. Shchukarev for help with XPS analysis.

■ REFERENCES

(1) Wang, H. L.; Gao, Q. M.; Hu, J. High Hydrogen Storage Capacity of Porous Carbons Prepared by Using Activated Carbon. *J. Am. Chem. Soc.* **2009**, *131*, 7016−7022.

(2) de la Casa-Lillo, M. A.; Lamari-Darkrim, F.; Cazorla-Amoros, D.; Linares-Solano, A. Hydrogen Storage in Activated Carbons and Activated Carbon Fibers. *J. Phys. Chem. B* **2002**, *106*, 10930−10934.

(3) Talyzin, A. V.; Klyamkin, S. Hydrogen Adsorption in C-60 at Pressures up to 2000 Atm. *Chem. Phys. Lett.* **2004**, *397*, 77−81.

(4) Hirscher, M.; Panella, B. Nanostructures with High Surface Area for Hydrogen Storage. *J. Alloys Compd.* **2005**, *404*, 399−401.

(5) Poirier, E.; Chahine, R.; Benard, P.; Cossement, D.; Lafi, L.; Melancon, E.; Bose, T. K.; Desilets, S. Storage of Hydrogen on Single-Walled Carbon Nanotubes and Other Carbon Structures. *Appl. Phys. A: Mater. Sci. Process.* **2004**, *78*, 961−967.

(6) Stadie, N. P.; Vajo, J. J.; Cumberland, R. W.; Wilson, A. A.; Ahn, C. C.; Fultz, B. Zeolite-Templated Carbon Materials for High-Pressure Hydrogen Storage. *Langmuir* **2012**, *28*, 10057−10063.

(7) Yushin, G.; Dash, R.; Jagiello, J.; Fischer, J. E.; Gogotsi, Y. Carbide-Derived Carbons: Effect of Pore Size on Hydrogen Uptake and Heat of Adsorption. *Adv. Funct. Mater.* **2006**, *16*, 2288−2293.

(8) Srinivas, G.; Zhu, Y. W.; Piner, R.; Skipper, N.; Ellerby, M.; Ruoff, R. Synthesis of Graphene-Like Nanosheets and Their Hydrogen Adsorption Capacity. *Carbon* **2010**, *48*, 630−635.

(9) Tozzini, V.; Pellegrini, V. Prospects for Hydrogen Storage in Graphene. *Phys. Chem. Chem. Phys.* **2013**, *15*, 80−89.

(10) Talyzin, A. V.; Jacob, A. Hydrogen Adsorption by Ball Milled C-60. *J. Alloys Compd.* **2005**, *395*, 154−158.

(11) Wang, J. C.; Kaskel, S. Koh Activation of Carbon-Based Materials for Energy Storage. *J. Mater. Chem.* **2012**, *22*, 23710−23725.

(12) Panella, B.; Hirscher, M.; Roth, S. Hydrogen Adsorption in Different Carbon Nanostructures. *Carbon* **2005**, *43*, 2209−2214.

(13) Poirier, E.; Chahine, R.; Bose, T. K. Hydrogen Adsorption in Carbon Nanostructures. *Int. J. Hydrogen Energy* **2001**, *26*, 831−835.

(14) Furukawa, H.; Yaghi, O. M. Storage of Hydrogen, Methane, and Carbon Dioxide in Highly Porous Covalent Organic Frameworks for Clean Energy Applications. *J. Am. Chem. Soc.* **2009**, *131*, 8875−8883.

(15) Langmi, H. W.; Ren, J. W.; North, B.; Mathe, M.; Bessarabov, D. Hydrogen Storage in Metal-Organic Frameworks: A Review. *Electrochim. Acta* **2014**, *128*, 368−392.

(16) Luzan, S. M.; Jung, H.; Chun, H.; Talyzin, A. V. Hydrogen Storage in Co-and Zn-Based Metal-Organic Frameworks at Ambient Temperature. *Int. J. Hydrogen Energy* **2009**, *34*, 9754−9759.

(17) Gadipelli, S.; Guo, Z. X. Graphene-Based Materials: Synthesis and Gas Sorption, Storage and Separation. *Prog. Mater. Sci.* **2015**, *69*, 1−60.

(18) Ghosh, A.; Subrahmanyam, K. S.; Krishna, K. S.; Datta, S.; Govindaraj, A.; Pati, S. K.; Rao, C. N. R. Uptake of H-2 and Co2 by Graphene. *J. Phys. Chem. C* **2008**, *112*, 15704−15707.

(19) Ma, L. P.; Wu, Z. S.; Li, J.; Wu, E. D.; Ren, W. C.; Cheng, H. M. Hydrogen Adsorption Behavior of Graphene above Critical Temperature. *Int. J. Hydrogen Energy* **2009**, *34*, 2329−2332.

(20) Klechikov, A.; Mercier, G.; Merino, P.; Blanco, S.; Merino, C.; Talyzin, A. V. Hydrogen Storage in Bulk Graphene-Related Materials. *Microporous Mesoporous Mater.* **2015**, *210*, 46−51.

(21) Chae, H. K.; Siberio-Perez, D. Y.; Kim, J.; Go, Y.; Eddaoudi, M.; Matzger, A. J.; O'Keeffe, M.; Yaghi, O. M. A Route to High Surface Area, Porosity and Inclusion of Large Molecules in Crystals. *Nature* **2004**, *427*, 523−527.

(22) Patchkovskii, S.; Tse, J. S.; Yurchenko, S. N.; Zhechkov, L.; Heine, T.; Seifert, G. Graphene Nanostructures as Tunable Storage Media for Molecular Hydrogen. *Proc. Natl. Acad. Sci. U. S. A.* **2005**, *102*, 10439−10444.

(23) Szabo, T.; Berkesi, O.; Forgo, P.; Josepovits, K.; Sanakis, Y.; Petridis, D.; Dekany, I. Evolution of Surface Functional Groups in a Series of Progressively Oxidized Graphite Oxides. *Chem. Mater.* **2006**, *18*, 2740−2749.

(24) He, H. Y.; Klinowski, J.; Forster, M.; Lerf, A. A New Structural Model for Graphite Oxide. *Chem. Phys. Lett.* **1998**, *287*, 53−56.

(25) You, S. J.; Luzan, S. M.; Szabo, T.; Talyzin, A. V. Effect of Synthesis Method on Solvation and Exfoliation of Graphite Oxide. *Carbon* **2013**, *52*, 171−180.

(26) Brodie, B. C. *Phil. Trans. R. Soc. Lond.* **1859**, *59*, 249−259.

(27) Hummers, W. S.; Offeman, R. E. Preparation of Graphitic Oxide. *J. Am. Chem. Soc.* **1958**, *80*, 1339−1339.

(28) Rezania, B.; Severin, N.; Talyzin, A. V.; Rabe, J. P. Hydration of Bilayered Graphene Oxide. *Nano Lett.* **2014**, *14*, 3993−3998.

(29) Talyzin, A. V.; Solozhenko, V. L.; Kurakevych, O. O.; Szabo, T.; Dekany, I.; Kurnosov, A.; Dmitriev, V. Colossal Pressure-Induced Lattice Expansion of Graphite Oxide in the Presence of Water. *Angew. Chem., Int. Ed.* **2008**, *47*, 8268−8271.

(30) Ruiz, J. C.; Macewan, D. M. C. Interlamellar Sorption Complexes of Graphitic Acid with Organic Substances. *Nature* **1955**, *176*, 1222−1223.

(31) Hofmann, U.; Frenzel, A. Quellung Von Graphit Und Die Bildung Der Graphitsaure. *Ber. Dtsch. Chem. Ges. B* **1930**, *63*, 1248.

(32) Talyzin, A. V.; Luzan, S. M.; Szabo, T.; Chernyshev, D.; Dmitriev, V. Temperature Dependent Structural Breathing of Hydrated Graphite Oxide in H(2)O. *Carbon* **2011**, *49*, 1894−1899.

(33) You, S. J.; Sundqvist, B.; Talyzin, A. V. Enormous Lattice Expansion of Hummers Graphite Oxide in Alcohols at Low Temperatures. *ACS Nano* **2013**, *7*, 1395−1399.

(34) You, S. J.; Luzan, S.; Yu, J. C.; Sundqvist, B.; Talyzin, A. V. Phase Transitions in Graphite Oxide Solvates at Temperatures near Ambient. *J. Phys. Chem. Lett.* **2012**, *3*, 812−817.

(35) Burress, J. W.; Gadipelli, S.; Ford, J.; Simmons, J. M.; Zhou, W.; Yildirim, T. Graphene Oxide Framework Materials: Theoretical Predictions and Experimental Results. *Angew. Chem., Int. Ed.* **2010**, *49*, 8902−8904.

(36) Srinivas, G.; Burress, J. W.; Ford, J.; Yildirim, T. Porous Graphene Oxide Frameworks: Synthesis and Gas Sorption Properties. *J. Mater. Chem.* **2011**, *21*, 11323−11329.

(37) Chan, Y.; Hill, J. M. Hydrogen Storage inside Graphene-Oxide Frameworks. *Nanotechnology* **2011**, *22*, 305403.

DOI: 10.1021/acs.jpcc.5b06402
J. Phys. Chem. C 2015, 119, 27179−27191

(38) Nicolai, A.; Sumpter, B. G.; Meunier, V. Tunable Water Desalination across Graphene Oxide Framework Membranes. *Phys. Chem. Chem. Phys.* **2014**, *16*, 8646−8654.
(39) Hwang, Y. H.; Bae, E. G.; Sohn, K. S.; Shim, S.; Song, X.; Lah, M. S.; Pyo, M. Sno2 Nanoparticles Confined in a Graphene Framework for Advanced Anode Materials. *J. Power Sources* **2013**, *240*, 683−690.
(40) Hung, W. S.; Tsou, C. H.; De Guzman, M.; An, Q. F.; Liu, Y. L.; Zhang, Y. M.; Hu, C. C.; Lee, K. R.; Lai, J. Y. Cross-Linking with Diamine Monomers to Prepare Composite Graphene Oxide-Framework Membranes with Varying D-Spacing. *Chem. Mater.* **2014**, *26*, 2983−2990.
(41) Tsoufis, T.; Katsaros, F.; Sideratou, Z.; Romanos, G.; Ivashenko, O.; Rudolf, P.; Kooi, B. J.; Papageorgiou, S.; Karakassides, M. A. Tailor-Made Graphite Oxide-Dab Poly(Propylene Imine) Dendrimer Intercalated Hybrids and Their Potential for Efficient Co2 Adsorption. *Chem. Commun.* **2014**, *50*, 10967−10970.
(42) Kumar, R.; Suresh, V. M.; Maji, T. K.; Rao, C. N. R. Porous Graphene Frameworks Pillared by Organic Linkers with Tunable Surface Area and Gas Storage Properties. *Chem. Commun.* **2014**, *50*, 2015−2017.
(43) Srinivas, G.; Burress, J.; Yildirim, T. Graphene Oxide Derived Carbons (Godcs): Synthesis and Gas Adsorption Properties. *Energy Environ. Sci.* **2012**, *5*, 6453−6459.
(44) Rouquerol, J.; Llewellyn, P.; Rouquerol, F. Is the Bet Equation Applicable to Microporous Adsorbents? *Stud. Surf. Sci. Catal.* **2006**, *160*, 49−56.
(45) De Weireld, G.; Frere, M.; Jadot, R. Automated Determination of High-Temperature and High-Pressure Gas Adsorption Isotherms Using a Magnetic Suspension Balance. *Meas. Sci. Technol.* **1999**, *10*, 117−126.
(46) Dolan, M. D.; McLennan, K. G.; Chandra, D.; Kochanek, M. A.; Song, G. Suppression of the Critical Temperature in Binary Vanadium Hydrides. *J. Alloys Compd.* **2014**, *586*, 385−391.
(47) Srenscek-Nazzal, J.; Kaminska, W.; Michalkiewicz, B.; Koren, Z. C. Production, Characterization and Methane Storage Potential of Koh-Activated Carbon from Sugarcane Molasses. *Ind. Crops Prod.* **2013**, *47*, 153−159.
(48) Cory, D. G.; Ritchey, W. M. Suppression of Signals from the Probe in Bloch Decay Spectra. *J. Magn. Reson.* **1988**, *80*, 128−132.
(49) Centeno, T. A.; Stoeckli, F. The Assessment of Surface Areas in Porous Carbons by Two Model-Independent Techniques, the Dr Equation and Dft. *Carbon* **2010**, *48*, 2478−2486.
(50) Boehm, H. P.; Scholz, W. Der Verpuffungspunkt Des Graphitoxids. *Z. Anorg. Allg. Chem.* **1965**, *335*, 74.
(51) Cote, A. P.; Benin, A. I.; Ockwig, N. W.; O'Keeffe, M.; Matzger, A. J.; Yaghi, O. M. Porous, Crystalline, Covalent Organic Frameworks. *Science* **2005**, *310*, 1166−1170.
(52) Gao, W.; Alemany, L. B.; Ci, L. J.; Ajayan, P. M. New Insights into the Structure and Reduction of Graphite Oxide. *Nat. Chem.* **2009**, *1*, 403−408.
(53) Erickson, K.; Erni, R.; Lee, Z.; Alem, N.; Gannett, W.; Zettl, A. Determination of the Local Chemical Structure of Graphene Oxide and Reduced Graphene Oxide. *Adv. Mater.* **2010**, *22*, 4467−4472.
(54) Wei, N.; Peng, X. S.; Xu, Z. P. Understanding Water Permeation in Graphene Oxide Membranes. *ACS Appl. Mater. Interfaces* **2014**, *6*, 5877−5883.
(55) Kowalczyk, P.; Holyst, R.; Terrones, M.; Terrones, H. Hydrogen Storage in Nanoporous Carbon Materials: Myth and Facts. *Phys. Chem. Chem. Phys.* **2007**, *9*, 1786−1792.

DOI: 10.1021/acs.jpcc.5b06402
J. Phys. Chem. C 2015, 119, 27179−27191